

CO-MOVING SPACE DENSITY OF X-RAY-SELECTED ACTIVE GALACTIC NUCLEI

J. D. SILVERMAN^{1,2,7}, P. J. GREEN¹, W. A. BARKHOUSE¹, R. A. CAMERON¹, C. FOLTZ⁵, B. T. JANNUZI⁴, D.-W. KIM¹, M. KIM¹, A. MOSSMAN¹, H. TANANBAUM¹, B. J. WILKES¹, M. G. SMITH⁶, R.C. SMITH⁶ AND P. S. SMITH³

Draft version May 23, 2019

ABSTRACT

For measurement of the AGN luminosity function and its evolution, X-ray selection samples all types of AGN and provides reduced obscuration bias in comparison with UV-excess or optical surveys. The apparent decline in optically-selected quasars above $z \sim 3$ may be strongly affected by such a bias. The Chandra Multi-wavelength Project (ChaMP) is characterizing serendipitously detected X-ray sources in a large number of fields with archival *Chandra* imaging. We present a measure of the co-moving space density using an initial sample of 311 AGNs found in 23 ChaMP fields ($\sim 1.8 \text{ deg}^2$) supplemented with 57 X-ray bright AGNs from the CDF-N and CDF-S. Above our X-ray flux ($f_{0.3-8.0 \text{ keV}} > 4 \times 10^{-15} \text{ erg cm}^{-2} \text{ s}^{-1}$) and optical magnitude ($r' < 22.5$) limits, we find 13 new AGN at $z > 3$. With this expanded sample, we detect a turnover in the co-moving space density for type 1 AGN with high luminosity ($\log L_X > 44.5$; units erg s^{-1} ; measured in the 0.3–8.0 keV band and corrected for Galactic absorption), similar to the optical surveys for the first time. We also confirm that at lower redshifts ($z < 1$) lower luminosity AGN ($\log L_X < 44.5$) are more prevalent by more than an order of magnitude. We combine the *Chandra* and *ROSAT* AGN samples to present a comprehensive measure of the space density of luminous type 1 AGN in the soft band (0.5–2.0 keV).

Subject headings: galaxies: active — quasars: general — X-rays: galaxies — surveys

1. INTRODUCTION

Optical surveys have measured the evolution of QSOs out to $z \sim 5$. The most dramatic feature found is the rise and fall of the co-moving space density with peak activity at $z \sim 2.5$. A systematic decrease in luminosity from $z \sim 2$ to the present is evident with very few bright QSOs in the local universe (e.g., Croom et al. 2004). This fading of the QSO population is attributed to a decreased fuel supply and/or fueling rate (e.g., Cavaliere & Vittorini 2000; Kauffmann & Haehnelt 2000). The dropoff in the space density at $z > 3$ (Warren, Hewitt, & Osmer 1994; Schmidt, Schneider, & Gunn 1995; Fan et al. 2001; Wolf et al. 2003) could represent the growth phase of supermassive black holes (SMBHs), possibly under a veil of obscuration (Fabian 1999).

It has become clear in the past decade that X-ray selection of AGN offers many benefits over detection methods in other wavebands. X-rays can penetrate large absorbing columns of gas which can effectively hide an accreting black hole in the optical. The existence of a significant, missed population of obscured AGN is required to explain the spectral shape of the Cosmic X-ray Background (CXRb; e.g., Gilli et al. 2001). The current generation of X-ray observatories (*Chandra*, *XMM-Newton*) are now able to probe the faint source population responsi-

ble for the bulk of the hard (2.0–8.0 keV) CXRB (e.g., Brandt et al. 2001; Rosati et al. 2002; Hasinger et al. 2001).

The evolution of X-ray emitting AGN has become quite intriguing with results from the hard X-ray surveys from *Chandra* (Cowie et al. 2003), *XMM-Newton* (Fiore et al. 2003) and *ASCA* (Ueda et al. 2003). There now exists a departure from the familiar rise of the co-moving space density of optically-selected QSOs with cosmic lookback time. The low luminosity ($L_{2.0-8.0 \text{ keV}} < 10^{44} \text{ erg s}^{-1}$) AGN tend to radiate at a later epoch ($z \sim 1$) than the luminous ($L_{2.0-8.0 \text{ keV}} > 10^{44} \text{ erg s}^{-1}$) QSOs. Semi-analytic models (Menci et al. 2004) posit that the more luminous QSOs illuminate early epochs when most of the massive galaxies are forming ($z > 2$), thereby inducing high accretion rates, whereas lower luminosity AGN activity is at a later period ($z < 2$) when most of the galaxies have fully assembled.

X-ray selected QSOs from *ROSAT* have hinted at a constant space density beyond a redshift of 2 (Miyaji et al. 2000). A higher space density of X-ray selected QSOs compared to that measured by optical surveys at high redshift ($z > 3$) could be evidence for an obscured state at early epochs. We can test this model (Fabian 1999) by measuring the luminosity function and co-moving space density of X-ray-selected AGN over a wide area to compile a significant sample at $z > 3$. Unfortunately, the *ROSAT* sample includes only 7 QSOs with $z > 3$. While the *Chandra* and *XMM-Newton* Deep field observations have great scientific merit, their narrow area provides only 4 high luminosity ($\log L_{0.3-8.0 \text{ keV}} > 44.5$) AGN at $z > 3$. A wider area survey is needed to compile a significant sample of high redshift and highly luminous QSOs.

2. CHANDRA MULTI-WAVELENGTH PROJECT

arXiv:astro-ph/0406330v1 14 Jun 2004

¹ Harvard-Smithsonian Center for Astrophysics, 60 Garden Street, Cambridge, MA 02138

² Astronomy Department, University of Virginia, P.O. Box 3818, Charlottesville, VA, 22903-0818

³ Steward Observatory, The University of Arizona, Tucson, AZ 85721

⁴ National Optical Astronomy Observatory, P.O. Box 26732, Tucson, AZ, 85726-6732

⁵ National Science Foundation, 4201 Wilson Blvd., Arlington, VA, 22230

⁶ Cerro Tololo Inter-American Observatory, National Optical Astronomical Observatory, Casilla 603, La Serena, Chile

⁷ jsilverman@cfa.harvard.edu

The ChaMP (Kim et al. 2004, Green et al. 2004) is carrying out a wide field X-ray survey encompassing $> 10 \text{ deg}^2$. Our ongoing optical imaging and spectroscopic followup of serendipitous X-ray sources in medium depth, archived *Chandra* fields is enabling us to measure the luminosity function out to $z \sim 5$. To date, we have amassed a sample of 358 AGN detected in the broad band (0.3–8.0 keV) in 23 ChaMP fields. We use the full *Chandra* energy range to take advantage of the high collecting area at soft energies to detect the faint, high redshift AGN. We present a preliminary measure of the co-moving space density of X-ray selected AGN out to $z \sim 4$. A complete presentation of the ChaMP X-ray luminosity function is forthcoming (Silverman et al. 2004, in preparation). We assume $H_0 = 70 \text{ km s}^{-1} \text{ Mpc}^{-1}$, $\Omega_\Lambda = 0.7$, and $\Omega_M = 0.3$ with the exception of Section 4.2.

3. AGN SELECTION AND COMPLETENESS

In these ChaMP fields, we find a diversity of objects (stars, AGN, clusters and galaxies), although 85% of them are attributed to an AGN. Green et al. (2004) present the X-ray and optical properties of X-ray sources detected in 6 fields with full details of the ChaMP optical followup program. We show the optical magnitude (r') as a function of 0.3–8.0 keV X-ray flux for the sources detected in 23 ChaMP fields (Figure 1 *top*). We only include sources within $12'$ of the aimpoint with greater than 9.5 net counts. Optical spectroscopic redshifts are available for all classified extragalactic objects: Broad Line AGN (BLAGN), Narrow Emission Line Galaxy (NELG), and Absorption Line Galaxy (ALG).

We set the X-ray flux ($f_{0.3-8.0 \text{ keV}} > 4 \times 10^{-15} \text{ erg cm}^{-2} \text{ s}^{-1}$) and optical magnitude ($r' < 22.5$) limits where we have identified $>30\%$ of the X-ray sources. Since the X-ray sources do not fully sample the $f_X - r'$ plane (Figure 1 *top*), we have implemented an adaptive binning scheme identical to that of (Sanders & Fabian 2001) to generate a completeness map as a function of X-ray and optical flux. We have included X-ray sources from the CDF-N (Brandt et al. 2001; Barger et al. 2002) and CDF-S (Szokoly et al. 2004) to boost the completeness at faint optical magnitudes. We create an array with 64×64 elements covering the $f_X - r'$ plane (Figure 1). The identified fraction f_{ID} is measured at each element as the number of identified objects divided by the number of X-ray sources. If 10 or more X-ray sources are in a single element, then we assign f_{ID} as the completeness level. We then increase the bin size by a factor of two. If the binned element has 10 or more objects, the individual elements not previously assigned an identified fraction are set to this value. This procedure occurs until the final binned element equals the size of the full array. In Figure 1 *bottom*, we plot the final completeness map.

To construct a pure AGN sample, we require the Galactic absorption corrected, rest frame 0.3–8.0 keV luminosity to exceed $10^{42} \text{ erg s}^{-1}$ thereby excluding any sources that contain a significant stellar or hot ISM component. We currently have only found AGN with broad emission lines beyond redshift of 1 in the ChaMP. Our current optical spectroscopic limit ($r' < 22.5$) precludes classification of objects with heavy optical extinction beyond this redshift, since a $\sim 5L_*$ elliptical has $r' \sim 23$ at $z \sim 1$. We detect many optical type 2 AGN with $L_X < 10^{44} \text{ erg s}^{-1}$ but no luminous ($L_X > 10^{44} \text{ erg s}^{-1}$) optical type 2

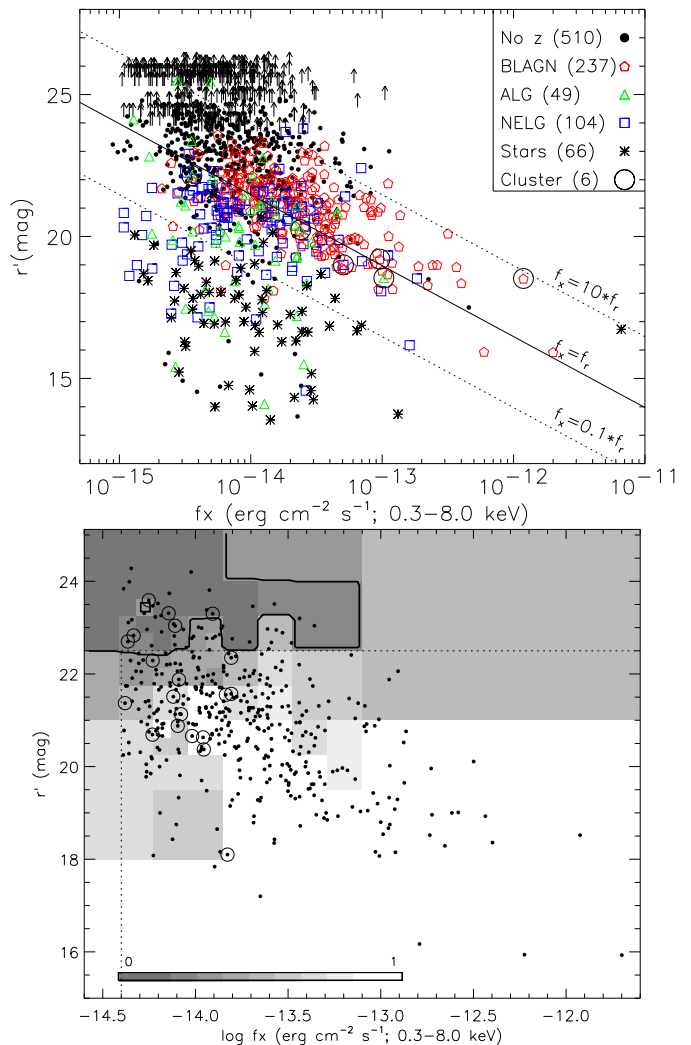


FIG. 1.— *top* Optical magnitude (r') vs. X-ray flux (0.3–8 keV) of X-ray sources found in 23 ChaMP fields. Optical spectroscopic classifications are indicated with the sample size. X-ray sources with no optical counterparts are shown by an arrow placed at the magnitude for a 5σ detection from our optical imaging. *bottom* Adaptively binned spectroscopic completeness map. The scale ranges from no identifications (0) to fully identified (1). Only spectroscopically identified AGN are shown with a black dot, those at $z > 3$ circled. Dashed lines show our chosen flux limits. A solid contour line has been overplotted to mark the 30% completeness level.

QSOs. We do find 6% of the BLAGN sample to be X-ray absorbed (Silverman et al. 2004). In Figure 1 *bottom*, we plot the location of the AGN, including those from the *Chandra* Deep Fields selected in the same manner, in the $f_X - r'$ plane. Though we do have 14 AGN (13 from ChaMP) at $z > 3$ above our flux limits, we are unable to include all AGN at high redshift in our sample due to low completeness at faint fluxes.

4. CO-MOVING SPACE DENSITY

We measure the co-moving space density using the $1/V_a$ method (Avni & Bahcall 1980) from our sample of 311 ChaMP AGN supplemented with 57 from the CDF N+S (Figure 2). The accessible volume V_a is determined for each individual object taking into consideration the X-ray and optical flux limits for that object. A correc-

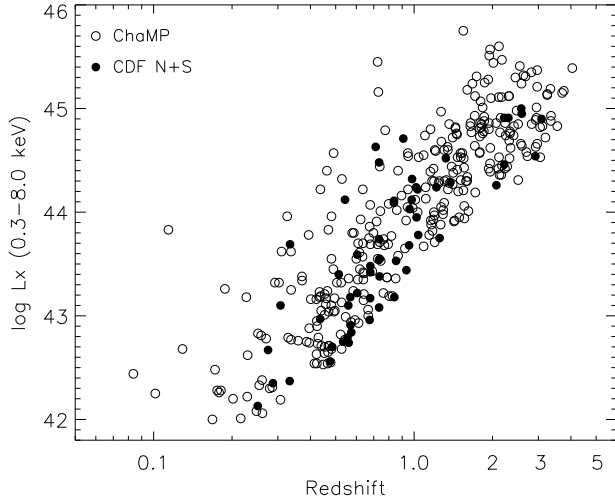


FIG. 2.— X-ray luminosity, redshift distribution of 368 AGN (311 ChaMP + 57 CDF N+S) with fluxes above our chosen limits.

tion factor (f_{ID}), determined from the location of an individual AGN in the $f_X - r'$ plane (Figure 1 *bottom*), is applied to compensate for the incompleteness in our spectroscopic identifications. Each AGN contributes $1/f_{\text{ID}}V_a$ to the space density in a specific luminosity and redshift interval. We estimate 1σ errors based on a Poisson distribution due to the small number of objects per redshift bin.

4.1. Broad band (0.3–8.0 keV)

In Figure 3, the co-moving number density is plotted for three luminosity bins. At $z < 1$, we confirm that the low luminosity ($\log L_X < 44.5$; units erg s^{-1}) AGN are over an order of magnitude more numerous than those with high luminosity (Fiore et al. 2003; Cowie et al. 2003; Ueda et al. 2003). The peak in space density appears to shift to lower redshift with decreasing luminosity. Keep in mind that we are limited in the detection of low luminosity AGN to $z < 1$ due to our bright spectroscopic limit (Section 3).

We have measured the rise and fall of the luminous ($\log L_X > 44.5$) AGN with a peak at $z \sim 2.5$. The ChaMP is the first X-ray survey to detect a turnover in the number density at high redshift. Thanks to a larger AGN sample (14) at $z > 3$, our results appear to disagree with those from *ROSAT* (Miyaji et al. 2000) which had only 5 AGN at these high luminosities. With *Chandra's* broad energy range, we can select an AGN sample in the soft band (0.5–2.0 keV) to directly compare with the *ROSAT* results (Section 4.2).

4.2. Soft band (0.5–2.0 keV): *Chandra* + *ROSAT*

The ChaMP AGN, supplemented by those in the *Chandra* Deep Fields, can be combined with the *ROSAT* sample (Miyaji et al. 2000) to measure the number density of AGN in the soft band with significant numbers of type 1 AGN over all redshifts. We use different cosmological parameters ($\Omega_M = 1$, $\Omega_\Lambda = 0$, $H_0 = 50 \text{ km s}^{-1} \text{ Mpc}^{-1}$) than previously to directly compare with the *ROSAT* and various optical surveys such as the 2dF (Croom et al. 2004), SDSS (Fan et al. 2001), and COMBO-17 (Wolf et al. 2003). The luminosity is calcu-

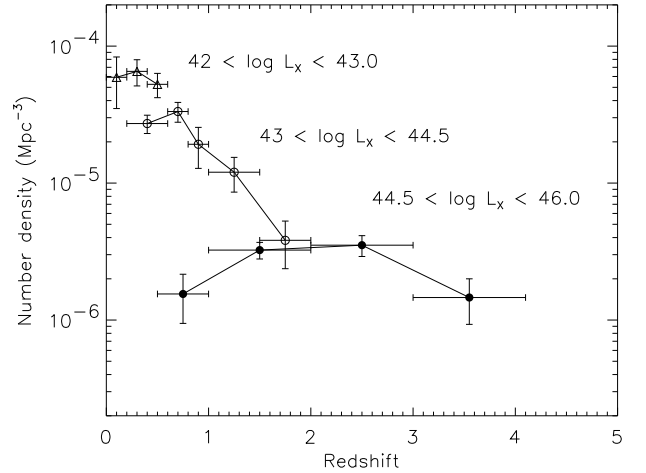


FIG. 3.— Co-moving space density of AGN selected in the broad (0.3–8.0 keV) band. Vertical bars are estimates of the 1σ error. Horizontal bars mark the redshift bin size.

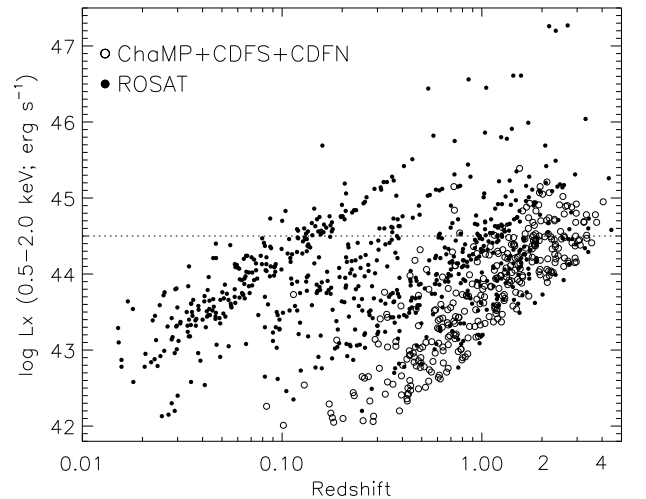


FIG. 4.— X-ray luminosity, redshift distribution of 1004 AGNs selected in the soft (0.5–2.0 keV) band with *ROSAT* and *Chandra*. The horizontal line shows our threshold for measuring the space density of highly luminous AGN.

lated in the observed frame (no k -correction) to compare with the *ROSAT* results (Miyaji et al. 2000). We have assembled a total of 1004 AGN with $L_{0.5-2.0 \text{ keV}} > 10^{42} \text{ erg s}^{-1}$, $f_X > 2 \times 10^{-15} \text{ erg cm}^{-2} \text{ s}^{-1}$, and $r' < 22.5$ (Figure 4). The ChaMP AGN boost the numbers at high redshift and lower luminosity due to *Chandra's* faint limiting flux.

In Figure 5, we plot the co-moving space density of the 217 most luminous ($\log L_{0.5-2.0 \text{ keV}} > 44.5$) X-ray emitting AGN. With these highly luminous AGN, we can compare the space density to past *ROSAT* results and optical surveys out to high redshift ($z < 5$). The number density of our combined sample is similar to the *ROSAT* results with $z < 3$. With the addition of AGN from 25 *Chandra* fields which reach similar depths ($\sim 10^{-15} \text{ erg cm}^{-2} \text{ s}^{-1}$) thereby reducing the effects of cosmic variance, we have more than doubled the number (12) of $z > 3$ luminous QSOs. We now see a decline in the space density. At $3 < z < 4.1$, our measurement is statistically inconsistent with *ROSAT* (Miyaji et al. 2000) at the 2σ level. To easily compare the space density evolution from

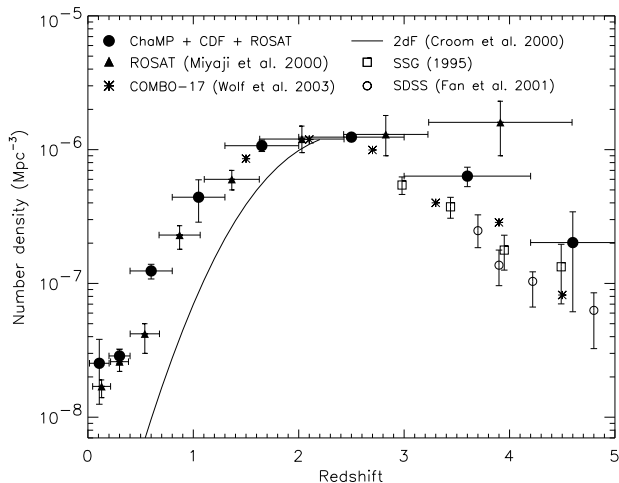


FIG. 5.— Co-moving space density of 217 *Chandra* + *ROSAT* AGN selected in the soft (0.5–2.0 keV) band with $\log L_X > 44.5$ compared to the optical surveys. The optical space densities have been scaled to match the X-ray points at $z = 2.5$ for ease of comparison.

optical surveys, in Figure 5, we have renormalized their curves to match the ChaMP at $z = 2.5$. For all but the COMBO-17 survey, optical curves have been scaled up by a factor of 3.7. COMBO-17 survey, which reaches much greater depths ($R < 24$) was scaled down ($7.7\times$). We find good agreement with a slight excess between the relative drop in the space density of the X-ray and optical surveys at $z > 2$. We are clearly detecting a decline in the space density of luminous AGN at high redshift.

Some caution must be taken in our comparison to optical surveys with vastly different magnitude limits. It is quite apparent that there is a discrepancy between the X-ray and 2dF optical survey at $z < 2$. This increase might be due to the fact that we probe AGN with absolute optical magnitudes ($M_i < -22$) fainter than the 2dF ($M_{b,r} < -24$) out to $z \sim 2$. The COMBO-17 survey which probes similar absolute magnitudes ($M_B < -22.2$) as the ChaMP has a higher space density than the 2dF at $z < 2$ which might reconcile the discrepancy.

5. CONCLUSION

We have measured the broad band (0.3–8.0 keV) co-moving space density using a sample of 368 X-ray emitting AGN detected by *Chandra* with the inclusion of

the absorbed AGN at $z < 1$ and unabsorbed AGN out to $z \sim 4$.

Our primary results are as follows:

- We confirm that the low luminosity AGN ($\log L_X < 44.5$) are more prevalent at lower redshifts than the higher luminosity AGN as seen by Cowie et al. (2003), Fiore et al. (2003), and Ueda et al. (2003).
- The space density of type 1, highly luminous ($\log L_X > 44.5$) X-ray selected AGN rises from the present epoch to a peak at $z \sim 2.5$ and then declines at $z > 3$. This behavior is similar to that of optically selected surveys. This is the first X-ray selected survey to detect a decline at high redshifts. The evolution is quite evident using a sample of 217 QSOs from *Chandra* and *ROSAT*.

Our results support a higher accretion rate and hence a more rapid depletion of fuel for the high luminosity AGN from $z \sim 2.5$ to the present epoch (Menci et al. 2004). At $z < 1$, the lower luminosity AGN are accreting at a lower rate and hence their evolution rate is quite slow compared to the more luminous AGN. At $z > 3$, the decline in the space density of highly luminous AGN represents the growth phase of supermassive black holes possibly during a period of rapid galaxy assembly. With the inclusion of obscured, highly luminous QSOs, X-ray surveys are well on the way to presenting a comprehensive view of AGN evolution.

We are greatly indebted to NOAO and the SAO TAC for their support of this work. We remain indebted to the staffs at Kitt Peak, CTIO, Las Campanas, Keck, FLWO, and MMT for assistance with optical observations. We thank Takamitsu Miyaji and Guenther Hasinger for providing us with the *ROSAT* AGN catalog.

We gratefully acknowledge support for this project under NASA under CXC archival research grants AR3-4018X and AR4-5017X. TLA, WAB, RAC, PJG, DWK, AEM, HT, and BW also acknowledge support through NASA Contract NASA contract NAS8-39073 (CXC).

REFERENCES

- Avni, Y., Bahcall, J.N. 1980, *ApJ*, 235, 694
 Barger, A.J. et al. 2002, *AJ*, 124, 1839
 Brandt, W.N. et al. 2001, *AJ*, 122, 2810
 Cavaliere, A. & Vittorini, V. 2000, *ApJ*, 543, 599
 Cowie, L.L., Barger, A.J., Bautz, M.W., Brandt, W.N., Garmire, G.P. 2003, *ApJ*, 584L, 57
 Croom, S.M., Smith, R.J., Boyle, B.J., Shanks, T., Miller, L., Outram, P.J., Loaring, N.S. 2004, *MNRAS*, 349, 1397
 Fabian, A. C. 1999, *MNRAS*, 308, 39
 Fan, X. et al. 2001, *AJ*, 121, 54
 Fiore, F. et al. 2003, *A&A*, 409, 79
 Gilli, R., Salvati, M., Hasinger, G. 2001, *A&A*, 366, 407
 Green, P.J. et al. 2004, *ApJS*, 150, 43
 Hasinger, G. et al. 2001, *A&A*, 365L, 45
 Kauffmann, G., Haehnelt, M. 2000, *MNRAS*, 311, 576
 Kim, D.-W. et al. 2004, *AJ*, 600, 59
 Menci, N., Fiore, F., Perola, G.C., Cavaliere, A. 2004, *ApJ*, 606, 58
 Miyaji, T., Hasinger, G., Schmidt, M. 2000, *A&A*, 353, 25
 Rosati, P. et al. 2002, *ApJ*, 566, 667
 Sanders, J.S., Fabian, A.C. 2001, *MNRAS*, 325, 178
 Schmidt, M., Schneider, D.P., Gunn, J.E. 1995, *AJ*, 110, 68
 Silverman, J.D. et al. 2004, *ApJ*, submitted
 Szokoly et al. 2004, *astro-ph/0312324*
 Ueda, Y., Akiyama, M., Ohta, K., Takamitsu, M. 2003, *ApJ*, 598, 886
 Warren, S.J., Hewett, P.C., Osmer, P.S. 1994, *ApJ*, 421, 412
 Wolf, C., Wisotzki, L., Borch, A., Dye, S., Kleinheinrich, M., Meisenheimer, K. 2003, *A&A*, 408, 499